



Análisis de la temperatura superficial en las áreas verdes de la ciudad de Durango, Durango

Analysis of the land surface temperature in the green areas of Durango city, state of Durango

Claudia Fabiola Reyes Rodríguez¹, Marcela Rosas Chavoya², Pablito Marcelo López Serrano^{3*}, José Ángel Prieto Ruiz¹, Félix Hinojosa Espinoza¹, Daniel José Vega Nieva¹

Fecha de recepción/Reception date: 4 de septiembre de 2023.

Fecha de aceptación/Acceptance date: 24 de noviembre de 2023.

¹Universidad Juárez del Estado de Durango, Facultad de Ciencias Forestales y Ambientales. México.

²Universidad Juárez del Estado de Durango, Instituto de Silvicultura e Industria de la Madera. México.

³Universidad Juárez del Estado de Durango, Programa Institucional de Doctorado en Ciencias Agropecuarias y Forestales. México.

*Autor para correspondencia; correo-e: p_lopez@ujed.mx

*Corresponding author; e-mail: p_lopez@ujed.mx

Abstract

The green areas in urban areas have provided a variety of ecosystem services which influence the quality of life of the inhabitants. The objective of this work was to analyze the effect of green areas on the Land Surface Temperature (*LST*) recorded by remote sensors in the city of *Durango, Durango*. The existing public and private green areas in the city were differentiated and the area in square meters per inhabitant was calculated. A classification by land use (urban, body of water, bare soil and green area) was carried out in order to analyze the *ST* derived from Landsat 8 satellite images and geographic information systems (QGIS), in addition a comparison of *ST* in three types of green areas (parks, squares and gardens, and ridges). The behavior of the *ST* was analyzed in two seasons of the year, in winter 2021 and spring 2022, identifying the areas with the highest incidence of temperature in two periods. The results indicate a lower *ST* in green areas compared to urban areas (concrete, construction and asphalt areas), as well as a regulatory trend in larger green areas (parks). The *ST* satellite product allowed to evaluate the temperature in spaces with vegetation within an urban area and it is shown that the larger the green area, the more thermal regulation exists in urban areas.

Key words: Urban green areas, heat islands, Landsat 8, QGIS, thermal regulation, land surface temperature.

Resumen

Las áreas verdes de las zonas urbanas contribuyen a la regulación térmica y por lo tanto al confort de la población. El objetivo del presente trabajo fue analizar el efecto de las áreas verdes en la temperatura superficial (*TS*) registrada mediante sensores remotos en la ciudad de *Durango, Durango*. Se diferenciaron las áreas verdes públicas y privadas existentes en la ciudad y se calculó la superficie en metros cuadrados por

habitante. Se realizó una clasificación por uso de suelo (urbano, cuerpo de agua, suelo desnudo y área verde) con el fin de analizar la *TS* derivada de imágenes del satélite *Landsat 8* y sistemas de información geográfica (*QGIS*); además, se hizo una comparación de *TS* en tres tipos de áreas verdes (parques, plazas, jardines y camellones). Se analizó el comportamiento de la *TS* en dos estaciones del año, en invierno de 2021 y primavera de 2022; a partir de lo cual se identificaron las zonas con mayor incidencia de temperatura en dos períodos. Los resultados indicaron una *TS* menor en las áreas verdes comparada con el uso de suelo urbano (zonas de concreto, construcción y asfalto), así como una tendencia regulatoria en las áreas verdes de mayor extensión (parques). El producto satelital *TS* permitió evaluar la temperatura en espacios con vegetación dentro de una zona urbana, y se demuestra que entre mayor es el área verde, más regulación térmica existe en las zonas urbanas.

Palabras clave: Áreas verdes urbanas, islas de calor, *Landsat 8*, *QGIS*, regulación térmica, temperatura superficial.

Introduction

Currently, the phenomenon of population migration has increased year after year. It is estimated that 5 % of the global population lives in urban areas and projections indicate that this figure will be 68 % by the year 2050 (ONU, 2020; Balsa-Barreiro *et al.*, 2021). Therefore, it is important to ensure well-being of the metropolitan population.

Urban areas have characteristics such as surfaces with little or no rainwater permeability due to the alteration of natural soils, which are replaced by concrete, asphalt, homes and buildings (Villalba, 2017). The increase in temperature associated with urban areas has economic, comfort, safety and population health repercussions (Aram *et al.*, 2019; Javadi and Nasrollahi, 2021). In this sense, it has been documented that green areas are related to the increase in well-being for inhabitants of urban areas. Specifically, the ability of vegetation to regulate the weather results in thermal comfort conditions for the population close to this type of infrastructure (Jabbar *et al.*, 2022).

Thus, green spaces in cities are a fundamental resource to promote the quality of life of the inhabitants. According to Rendón (2010), they provide ecological and social benefits that are linked to environmental and quality of life. In this context, the World Health Organization (WHO, 2012) establishes that an essential factor for access to a healthy life in urban areas is based on access to green spaces, which is why it is proposed that each neighborhood has 30 % of surface covered by tree canopy. This proposal, although ambitious, would guarantee important advantages to the physical and mental health of the population (Konijnendijk, 2021).

According to Ghosh and Das (2018), urban green areas can reduce the ambient temperature of nearby sites by up to 1 °C, allowing for cooler environments, with benefits associated with the reduction of ozone, which generally skyrockets in conditions of intense heat and increases the presence of heat islands. This type of thermal information from green areas can be studied with *in situ* information, by obtaining data to estimate the thermal sensation or ambient temperature (Aram et al., 2019), however, these methodologies entail high costs.

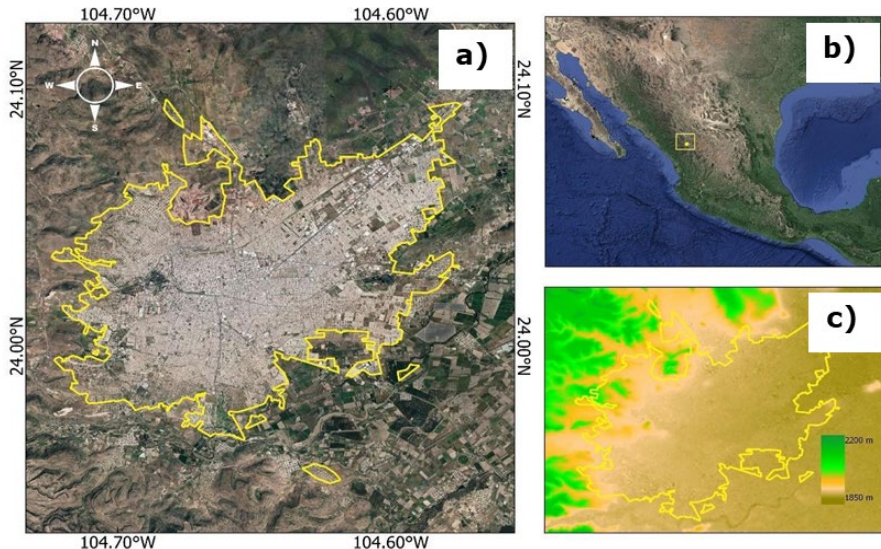
Some studies (Blancarte, 2016; Inevap, 2021) have described green areas, for example, in *Ciudad Victoria* in the state of *Durango*, work that, in spite of being valuable, is not enough, since it is still essential to generate information in this regard to strengthen the decision taking on the management and design of the city's green areas. Therefore, there is a need to implement new methodologies that allow characterizing, on the one hand, urban green areas and, on the other hand, the effect of these areas on urban ecology and social well-being. In this sense, the implementation of new sources of Surface Temperature (*ST*) information in urban areas derived from remote sensors is an alternative for the analysis of thermal conditions in urban environments, as well as the thermal effects of green areas (Sarricolea and Romero, 2010; Soto-Soto et al., 2020; Castro-Mendoza et al., 2022). The *TS* is the energy in the portion of the thermal infrared (*TIR*) that is emitted by the Earth's surface and is captured by the sensor (GUD, 2019). Under

this context, the objective of the present study was to analyze the effect of green areas on the surface temperature recorded by remote sensors in the city of *Durango, Durango, Mexico*.

Materials and Methods

Study area

The city of *Durango, Durango*, is located between 24°01'26" north and 104°40'13" west at an altitude of 1 890 m (Inegi, 2022), and is the capital of the state of *Durango, Mexico* (Figure 1). *Durango* city covers around 10 041 km² and has a population of 688 697 inhabitants with significant urban growth in recent years (Inegi, 2022). Average temperature of the coldest month is 1.7 °C and that of the hottest month 31 °C and 500 mm annual average rainfall.



a) Polygon of *Durango* city; b) Location of *Durango* city on the map of Mexico; c) Altitude differentiation in the polygon of *Durango* city.

Figure 1. Location of the study area.

Satellite information

Images were obtained from the Landsat 8 OLI/TIRS satellite of *Durango* city (Table 1). These images correspond to the winter 2021 and spring 2022 seasons and are available from the United States Geological Survey (USGS) (USGS, 2017). In this process, the Rstudio getSpatialData package (Kwok, 2018) was used.

Table 1. Characteristics of the spectral bands of the Landsat 8 satellite sensors.

Band name	Band	Band wavelength (μm)	Resolution (m)
-----------	------	-----------------------------------	----------------

Coastal spray	1	0.43-0.45	30
Blue	2	0.45-0.51	30
Green	3	0.53-0.59	30
Red	4	0.64-0.67	30
Near infrared (<i>NIR</i>)	5	0.85-0.88	30
Far infrared	6	1.57-1.65	30
Mid infrared	7	2.11-2.29	30
Panchromatic	8	0.50-0.68	15
Cirrus	9	1.36-1.38	30
Thermal infrared (<i>TIR</i>)	10	10.60-11.19	100
	11	-12.51	100

μm = Microns; m = Meters.

Source: USGS (2017).

Image preprocessing

In order to eliminate or reduce factors caused by atmospheric and topographic effects that could alter the results, the satellite images were preprocessed, which consisted of a radiometric and atmospheric correction with the help of the Semi Automatic Classification plug-in tool within the QGIS geospatial software version 3.14 (QGIS Development Team, 2020), using the Apparent Reflectance (TOA) technique, which allows transforming the digital levels (DL) to a normalized spectral scale (Chávez, 1988; López-Serrano *et al.*, 2016).

Coverage classification

A supervised classification was carried out to differentiate public and private green areas, based on the green areas of the city (cadastre) and areas such as parks, medians and gardens or squares were identified through remote sensors. The classification included green areas, urban (concrete, construction and asphalt areas), bare soil and bodies of water.

In addition, the surface area was calculated based on the area extension of each class. Thus, the following spectral index were estimated: Normalized Difference Vegetation Index (*NDVI*), which was mathematically developed by Rouse *et al.* (1974) to improve the visualization of the amount and plant photosynthetic activity on the surface of the Earth.

$$NDVI = \frac{(NIR - R)}{(NIR + R)} \quad (1)$$

Where:

NIR = Spectral band in the near infrared region

R = Band in the red region

The Normalized Difference Water Index (*NDWI*) was estimated using the technique proposed by McFeeters (1996) where the green portion band (GREEN) and the thermal infrared band (*NIR*) are used.

$$NDWI = \frac{G-NIR}{G+NIR} \quad (2)$$

Where:

NIR = Near infrared band reflectance values

G = Green portion band reflectance values

The Water Stress Index (*MSI*) allows identifying land surfaces with higher and lower moisture content. It takes values ranging from 0.4 to 2, and higher values are related to vegetation with water stress (Doraiswamy and Thompson, 1982).

$$MSI = \frac{SWIR}{NIR} \quad (3)$$

Where:

SWIR = Shortwave infrared band reflectance values

NIR = Near infrared band reflectance values

Object-based image analysis (OBIA) was performed on the images, through segmentation with the Orfeo Tool Box (OTB) algorithm, which consists of grouping contiguous pixels that have similar characteristics and results in a vector layer with as many polygons as the classification process obtain (Hossain and Chen, 2019). The training polygons represented at least 2 % of the total surface of the study area (Congalton and Green, 2008). Finally, the Random Forest classification algorithm was used using the Random Forest library (Liaw and Wiener, 2002) in Rstudio. In order to evaluate the accuracy of the supervised area classification, a confusion

matrix was generated to estimate the *Kappa* statistic, and the user accuracy and classification product were estimated (Liu et al., 2007). 20 % of the training pixels were used for the validation process.

Surface temperature

Surface temperature (*ST*) was estimated from band 10 for Landsat OLI/TIRS. Thus, the formula that provides the brightness temperature (*BT*) was applied through the Planck's law equation (Callejas et al., 2011), with which the pixel value of the thermal infrared band is transformed to values of temperature in Kelvin degrees.

$$TB = \frac{K_2}{\ln\left(\frac{K_1}{L_\lambda} + 1\right)} \quad (4)$$

$$TS = \frac{TB}{1 + \left(\lambda \times \frac{TB}{p}\right) \ln \epsilon} \quad (5)$$

Where:

TB = Brightness temperature

*K*₁ and *K*₂ = Calibration constants present in the metadata file of each image

L _{λ} = Spectral radiance obtained from the radiometric correction (TOA), followed by the calculation of surface temperature (Equation 2)

λ = Wavelength not converted to radiance values

ρ = 14 380 value

ε = Earth's surface emissivity

Earth's surface emissivity (Becker, 1987).

$$\varepsilon = 0.986 + 0.0004 \times Pv \quad (6)$$

$$Pv = \left(\frac{NDVI - NDVI_{min}}{NDVI_{max} - NDVI_{min}} \right)^2 \quad (7)$$

Where:

0.986 and 0.0004 = Constant values defined for each sensor

Pv = Vegetative portion estimated with the $NDVI$ values per pixel and the maximum and minimum $NDVI$ values present in the study area

Analysis of thermal data with respect to coverage

Once the supervised classification was carried out, the minimum and maximum temperatures were extracted for each of the classes. Of the types of soil (*i. e.*, green areas, bodies of water, urban soil, bare soil) and the main urban parks,

temperature was associated with the type of green area (park, squares and gardens, and medians). Finally, the city polygon was divided according to the cardinal points by zone in the polygon, in order to classify the city for the analysis of the *ST* according to the distribution of its green areas, starting from the *Catedral Basílica Menor de la Inmaculada Concepción* (Immaculate Conception Minor Basilica Cathedral), located in the center of the city, as a central point.

Results and Discussion

Public green areas, temperature and surface

The overall accuracy of the supervised classification was 97 % ($Kappa=0.95\%$), a result similar to that of Amini et al. (2022) in a study of the analysis of changes in urban land use and land cover with Landsat images and the Random Forest algorithm ($Kappa=93-97\%$). Table 2 shows the precision matrix, in which the producer precision is the specific probability of each class correctly classified, while the user precision is the possibility that a specific sample of each class represents the category in reality.

Table 2. Precision matrix.

Class	User precision	Producer precision
Urban	0.96	0.94

Water body	0.98	0.96
Bare ground	0.99	0.88
Green area	0.93	0.95
Overall Accuracy		97 %
<i>Kappa</i> Statistics		0.9522

The results of the surface of green area per inhabitant indicate that for public green areas in the city, according to the Municipal Directorate of Public Services for the year 2018 (Inegi, 2018), it was 2.49 m^2 per inhabitant, while for green areas obtained from INEGI (2005) was 2.03 m^2 . With this supervised classification methodology, a value of 10.56 m^2 per inhabitant was calculated. In this case, the green areas of public and private schools, sports and health institutions are considered, which were not included in the other alternatives. These results show that the green area per inhabitant in *Durango* city is below the recommendation for GEO Cities that establishes 12 m^2 per inhabitant as a reference value as an indicator of the quality of life in an urban area (PNUMA, 2011). Some studies carried out in the city record similar results, such as those of Blancarte (2016) who determined an average of 3.67 m^2 per inhabitant and, if private green areas are included, it is 5.06 m^2 per inhabitant. On the other hand, Inevap (2021) mentions 6.64 m^2 per inhabitant as an area coverage for the year 2021.

In Latin America, Romero (2017) obtained an average of 2.71 m^2 per inhabitant in the city of Lima, Peru, a reduced surface area that could have negative effects related to the degradation of ecosystems and detriment to the thermal comfort of the urban population (Ullah *et al.*, 2019). Frequently, the estimate of the square meters per inhabitant ratio is based on information on green areas recorded by the public administration, however, it is important to consider that such spaces with restricted access also offer environmental services to the population (Cilliers *et al.*, 2013).

Surface temperature distribution

Figure 2 illustrates the distribution of surface temperature (*ST*) in *Durango* city during winter for the different green areas in which a maximum temperature of 36 °C and a minimum of 13 °C is observed. Table 3 shows the average *ST* for winter, which is lower in larger green areas (parks) than in squares and gardens, followed by medians with a 0.93 °C difference greater than parks. The maximum temperature was 27.17 °C and the minimum 20.88 °C in squares and gardens. The results coincide with what has been reported by some authors about the negative relationship between the surface of the green area and the decrease in temperature, while the ridges, although small green areas, they should be considered as urban planning tools that achieve positive effects in lowering *ST* (Meyers et al., 2020).

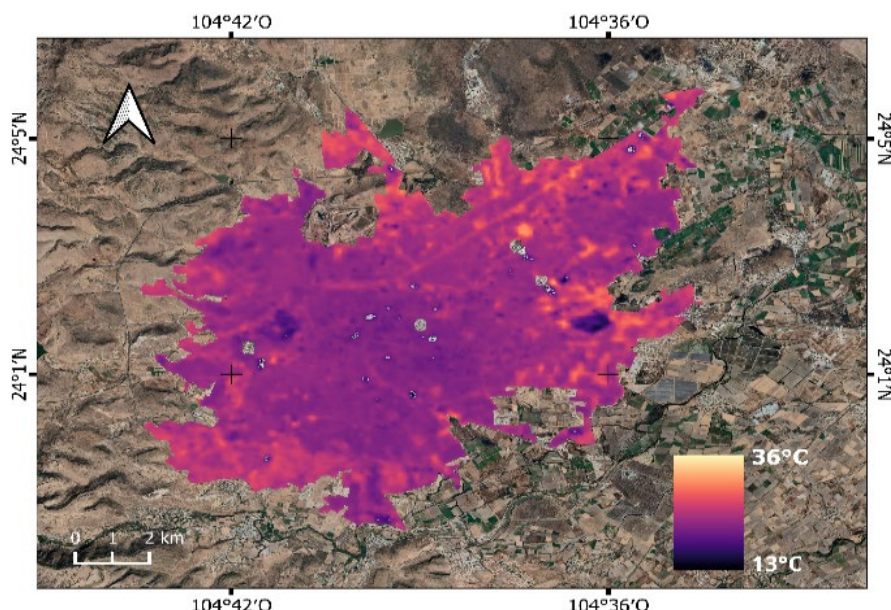


Figure 2. Map of the distribution of *ST* in *Durango* city, *Durango*, Mexico, during winter 2021.

Table 3. Superficial temperature in *Durango* city during winter.

Line tickets	Average <i>ST</i> (°C)	<i>ST</i> Maximum (°C)	<i>ST</i> Minimum (°C)
Parks (>20 ha)	21.77	22.51	21.03
Squares and gardens	23.11	27.17	20.88
Ridges	22.70	23.04	22.00

ST = Superficial temperature.

Likewise, Figure 3 shows the distribution of the *ST* in the city for the spring season, when the maximum temperature was 50 °C and the minimum was 24 °C. Table 4 shows that the average *ST* of *Durango* city for spring is lower (2.65 °C) in the largest green areas (parks) than in squares and gardens, followed by medians with a difference of 2.14 °C higher than in the parks. In the present study, a lower average *ST* was recorded in the median areas compared to squares and gardens. Although these results are contrasting with what was expected, an explanation could be related to the fact that the ridges receive constant irrigation from municipal services being easily accessible green areas.

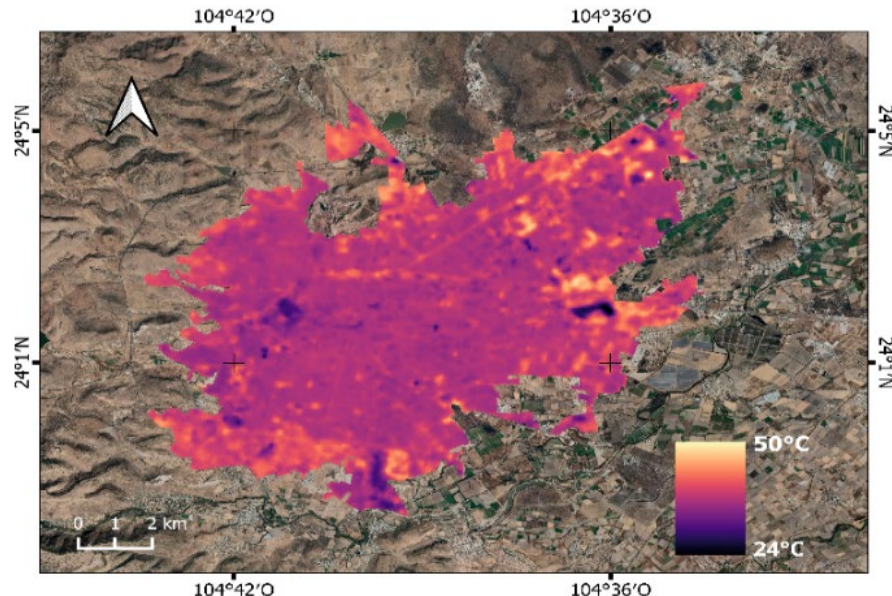


Figure 3. Map of the distribution of *ST* in *Durango* city, *Durango*, Mexico, during spring 2022.

Table 4. Superficial temperature in *Durango* city, *Durango*, Mexico, during spring.

Line tickets	Average <i>ST</i> (°C)	<i>ST</i> Maximum (°C)	<i>ST</i> Minimum (°C)
Parks (>20 ha)	33.84	35.52	32.17
Squares and gardens	36.49	42.75	34.17
Ridges	35.99	36.91	35.08

ST = Superficial temperatura.

It should be noted that the maximum temperature in April was 42.7 °C in squares and gardens, and the minimum was 32.17 °C in parks. When comparing both tables for the two seasons (winter and spring), the greatest difference on average was verified in squares and gardens with 7.5 °C between winter and spring; likewise, a difference between the two times of the year of up to 15.58 °C is recognized in the maximum temperature of squares and gardens.

The results show a considerable increase in the *ST* in spring, but highlights the thermal dynamics in the type of green areas by showing that in this season the ridges seem to have a lower temperature compared to the parks and gardens, which suggests a greater regulatory effect in this season. These data allow to infer that the ridges, despite their small surface area, are important thermal regulation mechanisms for the *Durango* city. It is recommended to allocate a greater amount of resources (economic and human) to the provision of municipal services for the maintenance of parks and gardens in spring, in order to increase the benefits of these places for its citizens.

Thermal effect by city section

When dividing the city polygon in order to analyze the thermal effect by zone (Figure 4), a constant temperature was observed that kept both periods (winter and spring) cooler with a temperature of 22.80 and 36.60 °C, respectively (Table 5). This is explained by the fact that the center of the city is where the largest extension of green areas is concentrated with 250.95 hectares, followed by the southern area with a similar trend in terms of temperature and 149.79 hectares of green areas (Figures 5 and 6). The southeast zone has the minimum extension of green areas and at the same time, a cooler temperature, since in this area there is a large coverage of crop lands, which can serve as thermal regulation areas while providing food provision for the nearby population (FAO, 2023).

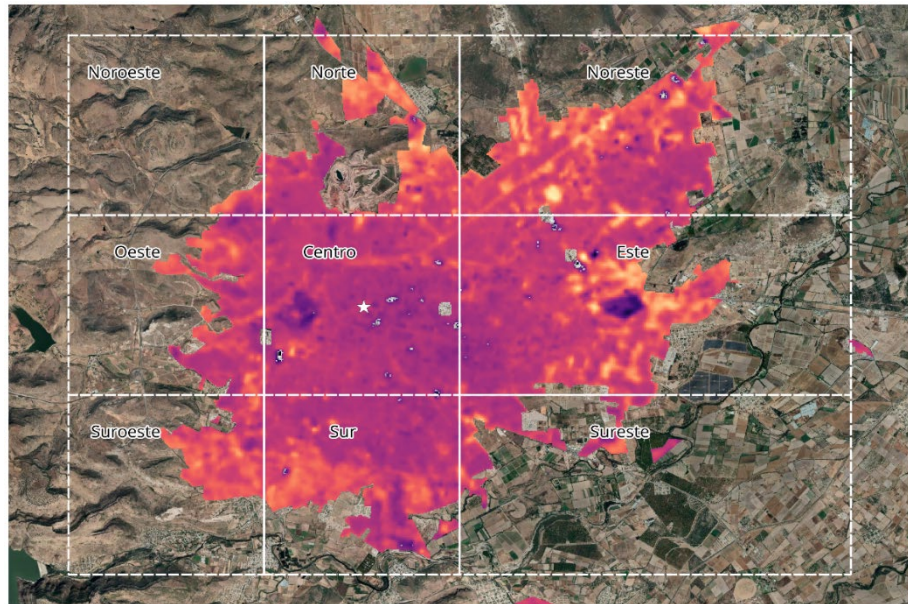


Figure 4. Temperature distribution map by area in *Durango* city, *Durango*, Mexico.

Table 5. Distribution of *ST* by area in winter and spring in *Durango* city, *Durango*, Mexico.

Zone	TS Inv. Prom.	TS Inv. Min.	TS Inv. Max.	TS Prim. Prom.	TS Prim. Min.	TS Prim. Max.	Extension (ha)
Center	22.8	13.85	29.07	36.6	27.67	44.06	250.95
South	23.11	17.13	28.27	36.89	29.33	45.29	149.79
Southeast	23.3	19.6	30.07	36.91	30.51	45.71	26.48
West	23.82	20.27	27.93	37.04	32.85	42.95	37.11
East	23.66	13.85	31.73	37.04	24.49	48.2	100.7
Northeast	24.51	15.75	31.45	37.55	24.93	49.29	36.3
Southwest	24.99	20.79	28.41	38.34	29.38	44.57	36.3
Northwest	24.38	20.68	28.31	38.47	35.29	42.41	79.17
North	24.67	19.02	30.9	38.61	28.14	45.67	47.11

TS Inv. Prom. = Average winter surface temperature; *TS Inv. Min.* = Minimum winter surface temperature; *TS Inv. Max.* = Maximum winter surface temperature;

TS Prim. Prom. = Average spring surface temperature; *TS Prim. Min.* = Minimum spring surface temperature; *TS Prim. Max.* = Maximum spring surface temperature.

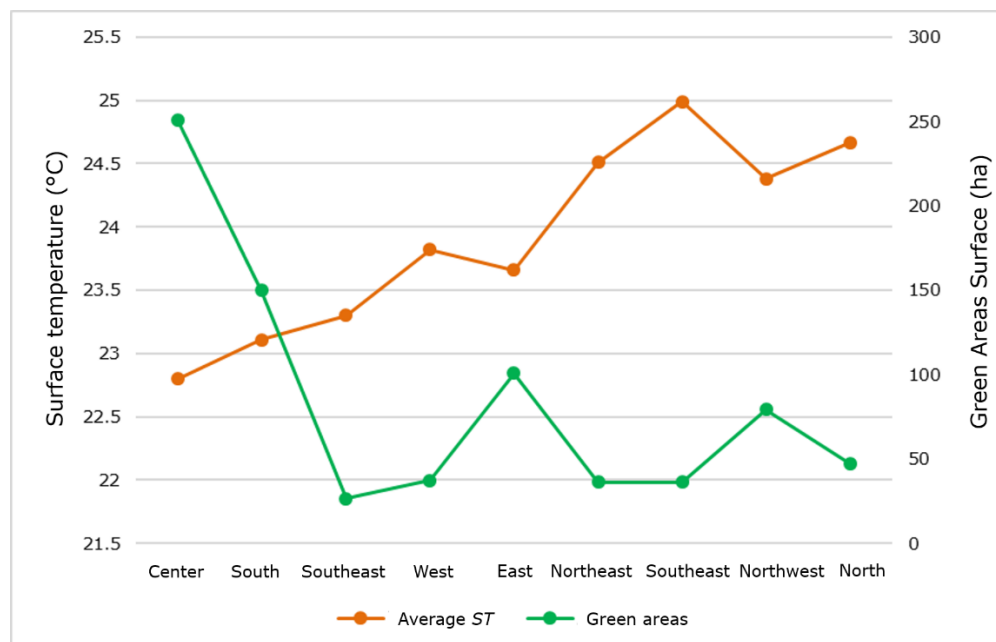


Figure 5. Temperature and green areas by zone in the winter period.

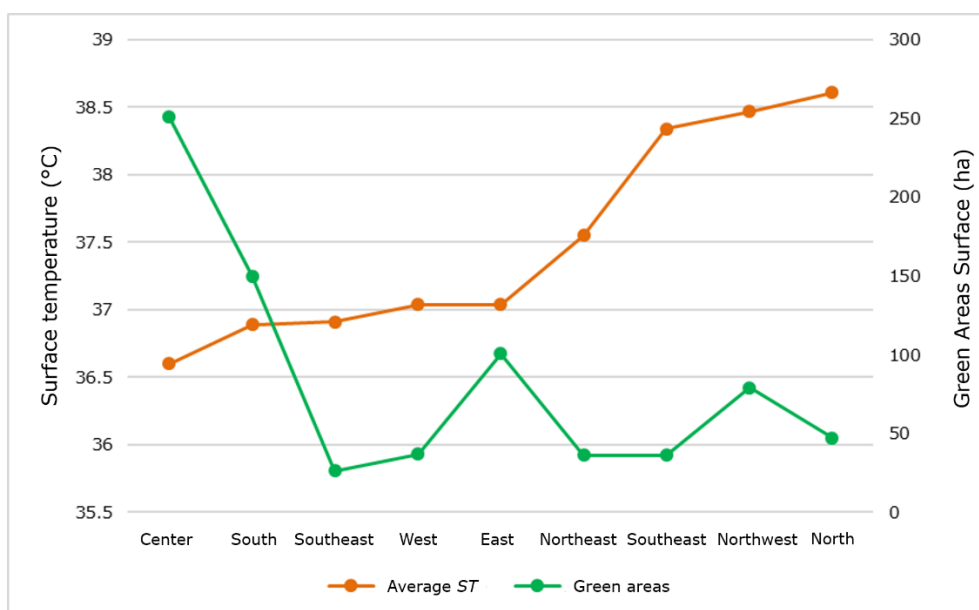


Figure 6. Temperature and green areas by zone in the spring period.

Finally, the areas that show a higher temperature are the northwest and the north, where the first has 79.17 ha and temperatures of 24.38 and 38.47 °C in each period, and the north part has only 47.11 ha of green areas and a temperature of 24.67 °C in winter (Figure 5) and 38.61 °C in spring (Figure 6).

The extension of green areas in a city has the ability to reduce the size and intensity of the urban heat island (UHI) through the evapotranspiration process considered as a natural cooling mechanism (Qiu et al., 2013). With these results it is observed that the greater the extension of the green area, the lower the temperature; this agrees with Kurbán et al. (2007) who indicate that a minimum surface with vegetation will produce an increase in relative humidity, but its scope will be limited to the area of the green space (GS) itself. Only by increasing this surface area to 2 500 m² will the scope of the effect cover the surrounding urban area, consequently, the *ST* of the surrounding urban areas will be influenced by the green areas: the greater their extension, the greater their regulatory effect.

On the other hand, the trend of apparent *ST* is higher in urban land than in green areas. Soto-Soto et al. (2020) obtained results that demonstrate this in continuous and discontinuous urban soils which present higher *ST* with average values of 23.2 °C and 21.6 °C respectively, unlike low vegetation with 20 °C and forest vegetation with 18.8 °C.

López et al. (2021) reached similar conclusions for the arid city of *Hermosillo, Sonora*, where they identified urban heat islands and urban oases using Landsat 8 image processing; the highest *ST* points were on bare soil with 44.2 °C and the urban oases varied in green areas and grasslands such as golf courses, which were estimated using the Moran index.

Conclusions

The *ST* satellite product derived from the Landsat 8 sensor made it possible to evaluate the temperature in spaces with vegetation within the city of *Durango* and it is shown that the larger the green area, the more thermal regulation exists in urban areas. The *ST* of such metropolis varies in the two seasons of the year according to its land uses (urban, bare soil, body of water and green areas). The largest difference in *ST* of urban and parks was 4.77 °C in spring and 3.03 °C in winter. This type of study allows us to identify the urban heat island in *Durango* city for the prevention of heat strokes that affect society.

Acknowledgements

The authors thank the Municipal Directorate of Public Services of the state of Durango for providing the necessary information.

Conflict of interest

The authors declare no conflict of interest.

Contribution by author

Claudia Fabiola Reyes Rodríguez: conception, writing and revision of the manuscript; Marcela Rosas Chavoya: review and collaboration in the analysis of the study; Pablito Marcelo López Serrano: conception, description of the methodology and manuscript review; José Ángel Prieto Ruiz and Félix Hinojosa Espinoza: review and coordination of the editing process; Daniel José Vega Nieva: review and correction of the manuscript.

Referencias

- Amini, S., M. Saber, H. Rabiei-Dastjerdi and S. Homayouni. 2022. Urban land use and land cover change analysis using Random Forest Classification of Landsat Time Series. *Remote Sensing* 14(11):2654. Doi: 10.3390/rs14112654.
- Aram, F., E. Higueras G., E. Solgi and S. Mansournia. 2019. Urban green space cooling effect in cities. *Heliyon* 5(4):e01339. Doi: 10.1016/j.heliyon.2019.e01339.
- Balsa-Barreiro, J., A. J. Morales and R. C. Lois-González. 2021. Mapping population dynamics at local scales using spatial networks. *Complexity* 2021:1-14. Doi: 10.1155/2021/8632086.
- Becker, F. 1987. The impact of spectral emissivity on the measurement of land surface temperature from a satellite. *International Journal of Remote Sensing* 8(10):1509-1522. Doi: 10.1080/01431168708954793.
- Blancarte S., R. H. 2016. La relación entre las áreas verdes y la calidad de vida en ambientes urbanos. Tesis de Maestría en Gestión Ambiental. Centro Interdisciplinario de Investigación para el Desarrollo Integral Regional (CIIDIR), Instituto Politécnico Nacional. Durango, Dgo., México. 113 p.
- Callejas, I. J. A., A. Santana de O., F. M. de Moura S., L. C. Durante, M. C. de J. Albuquerque N. and P. Zeilhofer. 2011. Relationship between land use/cover and surface temperatures in the urban agglomeration of Cuiabá-Várzea Grande, Central Brazil. *Journal of Applied Remote Sensing* 5(1):569-573. Doi: 10.1117/1.3666044.

- Castro-Mendoza, I., J. R. Valdez-Lazalde, G. Donovan, T. Martínez-Trinidad, F. O. Plascencia-Escalante and W. Vázquez-Morales. 2022. Does land-use affect the temperature distribution across the city of Tuxtla Gutiérrez, Chiapas, México? *Investigaciones Geográficas* (107):1-19. Doi: 10.14350/rig.60394.
- Chávez, P. S. 1988. An improved dark-object subtraction technique for atmospheric scattering correction of multispectral data. *Remote Sensing of Environment* 24(3):459-479. Doi: 10.1016/0034-4257(88)90019-3.
- Cilliers, S., J. Cilliers, R. Lubbe and S. Siebert. 2013. Ecosystem services of urban green spaces in African countries—perspectives and challenges. *Urban Ecosystems* 16:681-702. Doi: 10.1007/s11252-012-0254-3.
- Congalton, R. G. and K. Green. 2008. Assessing the accuracy of remotely sensed data. Principles and practices. CRC Press. Boca Raton, FL, United States of America. 183 p.
- Doraiswamy, P. C. and D. R. Thompson. 1982. A crop moisture stress index for large areas and its application in the prediction of spring wheat phenology. *Agricultural Meteorology* 27(1-2):1-15. Doi: 10.1016/0002-1571(82)90014-0.
- Food and Agriculture Organization of the United Nations (FAO). 2023. *Servicios ecosistémicos y biodiversidad*. <https://www.fao.org/ecosystem-services-biodiversity/background/regulatingservices/es/>. (17 de mayo de 2023).
- Ghosh, S. and A. Das. 2018. Modelling urban cooling island impact of green space and water bodies on surface urban heat island in a continuously developing urban area. *Modeling Earth Systems and Environment* 4:501-515. Doi: 10.1007/s40808-018-0456-7.
- Green Urban Data (GUD). 2019. *Temperatura superficial terrestre ¿afecta mi ciudad?* <https://www.greenurbandata.com/2019/02/20/temperatura-superficial>. (14 de marzo de 2023).
- Hossain, M. D. and D. Chen. 2019. Segmentation for Object-Based Image Analysis (OBIA): A review of algorithms and challenges from remote sensing perspective.

ISPRS Journal of Photogrammetry and Remote Sensing (150):115-134. Doi: 10.1016/j.isprsjprs.2019.02.009.

Instituto de Evaluación de Políticas Públicas del Estado de Durango (Inevap). 2021. Programa anual de evaluación 2021. Evaluación específica. Programa de crecimiento verde, incluyente, sostenible y sustentable, municipio de Durango. Inevap. Durango, Dgo., México. 116 p. <https://implandgo.gob.mx/IMPLAN/Sistema%20de%20Evaluaci%C3%B3n%20del%20Desempe%C3%B1o/Informe%20Final%20Programa%20Crecimiento%20Verde%202021.pdf>. (7 de septiembre de 2023).

Instituto Nacional de Estadística y Geografía (Inegi). 2018. Directorio Estadístico Nacional de Unidades Económicas 2018. Información para la actualización e incorporación de unidades económicas al DENU. Datos a noviembre de 2018 (DENU-2018). <https://www.inegi.org.mx/rnm/index.php/catalog/341/data-dictionary>. (15 de marzo de 2023).

Instituto Nacional de Estadística y Geografía (Inegi). 2022. Aspectos geográficos, Durango. Inegi. Aguascalientes, Ags., México. 44 p. https://www.inegi.org.mx/contenidos/app/areasgeograficas/resumen/resumen_10.pdf. (15 de marzo de 2023).

Instituto Nacional de Estadística, Geografía e Informática (INEGI). 2005. Cartografía Geoestadística Urbana 2005. Durango. INEGI. <https://www.inegi.org.mx/app/mapas/?t=710000000000000&tg=3604>. (6 de septiembre de 2023).

Jabbar, M., M. M. Yusoff and A. Shafie. 2022. Assessing the role of urban green spaces for human well-being: a systematic review. GeoJournal 87:4405-4423. Doi: 10.1007/s10708-021-10474-7.

Javadi, R. and N. Nasrollahi. 2021. Urban green space and health: The role of thermal comfort on the health benefits from the urban green space; a review study. Building and Environment 202:108039. Doi: 10.1016/j.buildenv.2021.108039.

- Konijnendijk, C. 2021. The 3-30-300 rule for urban forestry and greener cities. Biophilic Cities Journal 4(2):1-2. https://static1.squarespace.com/static/5bbd32d6e66669016a6af7e2/t/6101ce2b17dc51553827d644/1627508274716/330300+Rule+Preprint_7-29-21.pdf. (5 de septiembre de 2023).
- Kurbán, A., A. Papparelli, M. Cúnsulo, E. Montilla y E. Ríos. 2007. Espacios verdes y variación de la humedad relativa en entornos urbanos áridos. In: Saravia, L., R. Echazú, R. Abalone, R. Caso, ... y M. Tamasi (Comps.). XXX Congreso de la Asociación Argentina de Energías Renovables y Medio Ambiente (Asades). Asades. San Luis, D, Argentina. pp. 1-6. http://sedici.unlp.edu.ar/bitstream/handle/10915/94022/Documento_completo.pdf?sequence=1. (6 de mayo de 2023).
- Kwok, R. 2018. Ecology's remote-sensing revolution. Nature 556:137-138. <https://www.nature.com/articles/d41586-018-03924-9>. (5 de septiembre de 2023).
- Liaw, A. and M. Wiener. 2002. Classification and Regression by randomForest. R News 2-3:18-22. <https://cogns.northwestern.edu/cbmg/LiawAndWiener2002.pdf>. (5 de septiembre de 2023).
- Liu, C., P. Frazier and L. Kumar. 2007. Comparative assessment of the measures of thematic classification accuracy. Remote Sensing of Environment 107(4):606-616. Doi: 10.1016/j.rse.2006.10.010.
- López G., F. M, L. A. Navarro N., R. E. Díaz C. y J. Navarro-Estupiñán. 2021. Cobertura vegetal y la distribución de islas de calor/oasis urbanos en Hermosillo, Sonora. Frontera Norte 33:1-32. Doi: 10.33679/rfn.v1i1.2088.
- López-Serrano, P. M., J. J. Corral-Rivas, R. A. Díaz-Varela, J. G. Álvarez-González and C. A. López-Sánchez. 2016. Evaluation of radiometric and atmospheric correction algorithms for aboveground forest biomass estimation using Landsat 5 TM data. Remote Sensing 8(5):369. Doi: 10.3390/rs8050369.

- McFeeters, S. K. 1996. The use of the Normalized Difference Water Index (NDWI) in the delineation of open water features. International Journal of Remote Sensing 17(7):1425-1432. Doi: 10.1080/01431169608948714.
- Meyers, J., A. Langston, D. Devereux and B. Lin. 2020. Mapping land surface temperatures and heat-health vulnerability in Darwin. Commonwealth Scientific and Industrial Research Organisation (CSIRO). Canberra, ACT, Commonwealth of Australia. https://research.csiro.au/darwinlivinglab/wp-content/uploads/sites/278/2020/12/CSIRO_Mapping_LST__Heat_Health_Vulnerability_In_Darwin_Final.pdf. (28 de septiembre de 2023).
- Organización de las Naciones Unidas (ONU). 2020. *Día Mundial de las Ciudades: Las comunidades son la raíz de las urbes sostenibles*. <https://news.un.org/es/story/2020/10/1483282>. (3 de marzo de 2023).
- Programa de las Naciones Unidas para el Medio Ambiente (PNUMA). 2011. Informe Anual 2010. Síntesis del año. PNUMA. Nairobi, KE, Kenia. 124 p. https://www.iri.edu.ar/publicaciones_ir/ir/anuario/cd_anuario_2011/Mayd/Programa%20de%20las%20Naciones%20Unidas%20para%20el%20Medio%20Ambiente%20-%20Informe%202010.pdf. (28 de septiembre de 2023).
- QGIS Development Team. 2020. Geographic Information System version 3.14. Open Source Geospatial Foundation Project. <http://qgis.osgeo.org>. (26 de enero de 2020).
- Qiu, G. Y., H. Y. Li, Q. T. Zhang, W. Chen, X. J. Liang and X. Z. Li. 2013. Effects of evapotranspiration on mitigation of urban temperature by vegetation and urban agriculture. Journal of Integrative Agriculture 12(8):1307-1315. Doi: 10.1016/S2095-3119(13)60543-2.
- Rendón G., R. E. 2010. Espacios verdes públicos y calidad de vida. In: Centre de Política de Sòl i Valoracions y Universidad Autónoma de Baja California (Edits.). Memorias del 6º Congreso Internacional Ciudad y Territorio Virtual. Centre de Política de Sòl i Valoracions y Universidad Autónoma de Baja California. Mexicali,

BC, México. pp. 1-14. <https://upcommons.upc.edu/handle/2099/12860>. (14 de marzo de 2023).

Romero B., R. 2017. *Lima tiene un déficit de 56 millones de metros cuadrados de áreas verdes*. <https://rpp.pe/politica/actualidad/lima-tiene-un-deficit-de-61-millones-de-metros-cuadrados-en-areas-verdes-noticia-1021931>. (6 de septiembre de 2023).

Rouse, J. W., R. H. Haas, J. A. Schell and D. W. Deering. 1974. Monitoring vegetation systems in the Great Plains with ERTS. In: Freden, C. S. and E. P. Mercanti (Edits.). Proceedings of the Third ERTS-1 Symposium. National Aeronautics and Space Administration. Washington, DC, United States of America. pp. 309-317.

Sarricolea E., P. y H. Romero A. 2010. Análisis de los factores condicionantes sobre las temperaturas de emisión superficial en el área metropolitana de Valparaíso, Chile. ACE: Architecture, City and Environment 5(14):79-96. Doi: 10.5821/ace.v5i14.2507.

Soto-Soto, J. E., J. Garzón-Barrero y G. Jiménez-Cleves. 2020. Análisis de islas de calor urbano usando imágenes Landsat: caso de estudio Armenia-Colombia 1996-2018.

Revista Espacios 41(8):9.

<https://www.revistaespacios.com/a20v41n08/a20v41n08p09.pdf>. (5 de septiembre de 2023).

Ullah, S., K. Ahmad, R. U. Sajjad, A. M. Abbasi, A. Nazeer and A. A. Tahir. 2019. Analysis and simulation of land cover changes and their impacts on land surface temperature in a lower Himalayan region. Journal of Environmental Management 245:348-357. Doi: 10.1016/j.jenvman.2019.05.063.

United States Geological Survey (USGS). 2017. Landsat 8. Discover the science that our satellites bring to you. <https://geonarrative.usgs.gov/landsat-8/>. (14 de marzo de 2023).

Villalba M., J. C. 2017. Las áreas verdes urbanas y su relación con la infiltración de agua al subsuelo como servicio ambiental en Xalapa, Veracruz. Tesis de

Maestría en Desarrollo Regional Sustentable. El Colegio de Veracruz. Xalapa de Enríquez, Ver., México. 111 p.

World Health Organization (WHO). 2012. Health indicators of sustainable cities in the context of the Rio+20. UN Conference on Sustainable Development. https://www.who.int/docs/default-source/environment-climate-change-and-health/sustainable-development-indicator-cities.pdf?sfvrsn=c005156b_2. (6 de septiembre de 2023).



Todos los textos publicados por la **Revista Mexicana de Ciencias Forestales** –sin excepción– se distribuyen amparados bajo la licencia *Creative Commons 4.0 Atribución-No Comercial (CC BY-NC 4.0 Internacional)*, que permite a terceros utilizar lo publicado siempre que mencionen la autoría del trabajo y a la primera publicación en esta revista.